19-hydroxyisovoacangine, and it probably was formed by reaction between acetone and the latter alkaloid. The spectral properties of XIV were consistent with those of V. In particular, XIV showed peaks at m/e 192, 136, and 122 in its mass spectrum, as did V, and both compounds also showed strong peaks in their IR spectra at about 1720 cm^{-1} for the ester and ketonic carbonyl absorptions. It is concluded, therefore, that the new ketonic alkaloid possesses Structure V, in which the stereochemistry at C-19 is unknown. It is likely that this alkaloid also was formed as an artifact by reaction of 19-hydroxyconodurine with traces of acetone present in the methanol during extraction or chromatography.

REFERENCES

(1) M. Hesse, "Indolalkaloide in Tabellen," Springer-Verlag, Berlin, West Germany, 1964 and 1968.

(2) I. M. Jakovljevic, L. D. Seay, and R. W. Shaffer, J. Pharm. Sci., 53, 553 (1964).

(3) D. G. I. Kingston and B. T. Li, J. Chromatogr., 104, 431 (1975).

(4) T. R. Govindachari, B. S. Joshi, A. K. Saksena, S. S. Sathe, and N. Viswanathan, Chem. Commun., 1966, 97.

(5) N. Neuss, "Physical Data of Indole and Dihydroindole Alkaloids," Eli Lilly, Indianapolis, Ind., 1964.

(6) M. Hesse, in "Progress in Mass Spectrometry," vol. 1, H. Budzikiewicz, Ed., Verlag Chemie, Weinheim, West Germany, 1974.

(7) W. E. Meyer, J. A. Coppola, and L. Goldman, J. Pharm. Sci., 62, 1199 (1973).

(8) U. Renner and H. Fritz, Tetrahedron Lett., 1964, 283.

(9) M. P. Cava, S. K. Talapatra, J. A. Weisbach, B. Douglas, R. F. Raffauf, and J. L. Beal, ibid., 1965, 931.

(10) G. H. Svoboda, N. Neuss, and M. Gorman, J. Am. Pharm. Assoc., Sci. Ed., 48, 659 (1959).

(11) M. Gorman and J. Sweeny, Tetrahedron Lett., 1964, 3105.

(12) N. R. Farnsworth, W. D. Loub, R. N. Blomster, and M. Gorman, J. Pharm. Sci., 53, 1558 (1964).

(13) U. Renner, D. A. Prins, and W. G. Stoll, Helv. Chim. Acta, 42, 1572 (1959).

(14) G. Büchi, R. E. Manning, and S. A. Monti, J. Am. Chem. Soc., 86, 4631 (1964).

(15) G. B. Guise, E. Ritchie, and W. C. Taylor, Aust. J. Chem., 18, 1279 (1965).

(16) D. W. Thomas and K. Biemann, J. Am. Chem. Soc., 87, 5447 (1965).

(17) D. G. I. Kingston, J. T. Bursey, and M. M. Bursey, Chem. Rev., 74, 215 (1974).

(18) V. C. Agwada, Y. Morita, U. Renner, M. Hesse, and H. Schmid, Helv. Chim. Acta, 58, 1001 (1975).

Physiologically Based Pharmacokinetic Model for Digoxin Distribution and Elimination in the Rat

LESTER I. HARRISON * and MILO GIBALDI *

Abstract □ A plasma flow rate-limited pharmacokinetic model was developed to describe the distribution of digoxin to the heart, liver, kidneys, skeletal muscle, and GI tract in the rat. The model also provides for renal, hepatic (metabolic and biliary), and GI clearance as well as for biliary and GI secretion and GI reabsorption of digoxin. Predicted concentrations of digoxin in the heart, liver, skeletal muscle, and plasma were consistent with experimental observations in conscious rats after an intravenous dose. The model was extended to describe digoxin concentrations in the plasma of bile duct-ligated rats and ureter-ligated rats, simply by modifying appropriate clearance parameters. Excellent agreement was obtained between predicted and observed urinary excretion rates of digoxin for 12 hr after an intravenous dose to normal and bile duct-ligated rats.

Keyphrases □ Digoxin—pharmacokinetic model for distribution and elimination, effect of ligation of bile duct or ureter, rats □ Pharmacokinetics—digoxin, model for distribution and elimination, effect of ligation of bile duct or ureter, rats □ Distribution, tissue—digoxin, pharmacokinetic model, effect of ligation of bile duct or ureter, rats □ Elimination—digoxin, pharmacokinetic model, effect of ligation of bile duct or ureter, rats □ Cardiotonic agents—digoxin, pharmacokinetic model for distribution and elimination, effect of ligation of bile duct or ureter, rats

Compartment models to describe the pharmacokinetics of drug disposition are usually developed by curve fitting plasma concentration data with multiexponential equations. Due to the limitations of this approach, usually no representation more complex than a two-compartment open model is justified to describe the time course of drug concentrations in plasma. In almost all instances, compartment volumes and transfer constants have no anatomical or physiological reality. Moreover, these models are very species dependent. Although classical pharmacokinetic models have many clinical applications, the amount of basic information they provide is intrinsically limited.

In recent years, there has been considerable interest in the development of anatomically and physiologically realistic pharmacokinetic models for drug disposition based on organ blood or plasma flows and volumes (1). In principle, these models permit the prediction of drug concentrations in any target tissue at any time and may provide considerable insight to drug dynamics. Furthermore, drug distribution in certain pathophysiologic conditions may be simulated by altering estimates of organ blood flow (2, 3). Perhaps most important, physiologically based models can be scaled to apply to several species (4). Thus, the large data base required to develop a physiological pharmacokinetic model may be collected in a laboratory animal

and scaled to apply to humans. This approach has been investigated with thiopental (5), methotrexate (6), cytarabine (7), lidocaine (2), and sulfobromophthalein (8).

The present report describes the development of a physiologically based pharmacokinetic model for digoxin distribution and elimination in normal rats and the application of suitably modified forms of this model to describe the time course of digoxin concentrations in the plasma of rats with total obstruction of the common bile duct or ureters.

EXPERIMENTAL

The drugs, chemicals, and surgical procedures used were described previously (9). Briefly, male Sprague–Dawley rats, 300–400 g, were cannulated via the jugular vein. The common bile duct in one group and the ureters in a second group of rats were ligated. The bile duct and ureters of control animals also were isolated and traumatized, but no ligations were made. All animals were allowed to recover overnight with food and water available and were conscious during all experiments.

For the intravenous bolus studies, the rats were injected through the cannula with a 1-mg/kg dose of digoxin containing 3 µg of ^{3}H-digoxin[1], specific activity 6.19 Ci/mmole. Blood samples were withdrawn through the cannula at various times after dosing and collected in heparinized centrifuge tubes. Urine was collected at timed intervals. Control animals were sacrificed at 5, 11, 22, 40, 60, and 94 min after digoxin administration by an injection of air into the jugular vein. The heart, liver, and a portion of skeletal muscle (right anterior thigh) were excised, rinsed well with ice-cold saline, blotted, weighed, and frozen until analyzed for drug content.

For the infusion studies, a loading dose of 0.12 mg, followed by a constant-rate infusion of 0.036 mg of digoxin in 1.1 ml of saline/hr, was administered to control rats and to bile duct-ligated rats. All injection solutions contained ^{3}H-digoxin at the same specific activity. Based on the data collected after the intravenous bolus injection of digoxin, this infusion rate was expected to yield steady-state plasma digoxin concentrations of about 100 ng/ml.

The infusion was interrupted briefly at 10 hr to obtain a blood sample and terminated at 12 hr after removal of a second blood sample. The similarity of digoxin concentrations in these samples indicated that steady state with respect to plasma digoxin levels was attained within 10 hr. Urine and feces were collected continuously during infusion. The animals were sacrificed right after the infusion was terminated. The heart, liver, kidneys, skeletal muscle, and GI tract were excised, rinsed, and weighed. These tissues, as well as the carcass, were frozen until analyzed for drug content.

Plasma and urine samples were extracted and chromatographed to separate digoxin from its metabolites as described previously (9). Tissue samples were homogenized with a five- to 10-fold excess of 40% ethanol in an all-glass tissue grinder. The carcass was skinned and homogenized in a small meat grinder.

Five milliliters of each homogenate was extracted first with a two- to threefold excess of chloroform and then twice with chloroform–methanol (1:1). The extracts were reduced under vacuum and chromatographed. In addition, 200–400 mg of each homogenate was combusted in a tissue oxidizer[2] to determine radioactivity. The efficiency of combustion based on ^{3}H-spiked samples was 98%.

The chromatography system consisted of chloroform–acetic acid–ethyl acetate (5:5:90). Spots were identified by comparison to standards, scraped into vials, and counted in a dioxane-based scintillator as described previously (9). Recovery of radioactivity from ^{3}H-spiked tissues and urine was better than 90% in all cases.

RESULTS AND DISCUSSION

Intravenous Bolus Studies—The time course of digoxin concentrations in the plasma was biexponential in all cases. Figures 1, 2, and 3 show typical results in a control, bile duct-ligated, and ureter-ligated rat, respectively. Plasma digoxin concentration–time curves were quite similar in control rats and in rats with ligated bile ducts. The data from
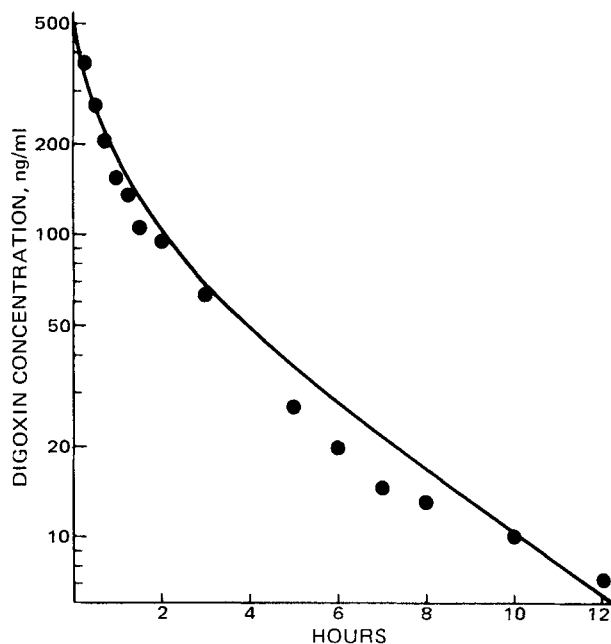
[1] New England Nuclear Corp., Boston, Mass.
[2] Packard Instruments, Downers Grove, Ill.

Figure 1—*Predicted (—) and observed (●) plasma digoxin concentrations after a 1-mg/kg iv injection to a control rat.*

rats with ligated ureters indicated a longer half-life and a reduced total clearance of digoxin compared to those observed in control rats.

Digoxin concentrations in heart, skeletal muscle, and liver of control rats are shown in Fig. 4. The drug levels in the heart and muscle were comparable to plasma digoxin levels. Digoxin concentrations in the liver were much greater than those in the plasma, suggesting considerable binding of the drug in this tissue.

Infusion Studies—Steady-state digoxin concentrations in various tissues after a 12-hr constant-rate infusion in normal rats are shown in Table I. This table also includes the tissue-to-plasma partition coefficients observed in each animal.

Digoxin was taken up efficiently by the GI tract and the liver. About 80% of the digoxin in the GI tract was found in the small intestine and cecum; less than 1% was in the stomach. High digoxin concentrations in these organs also were found in the dog (10). In humans, digoxin is poorly concentrated by the GI tissues (11).
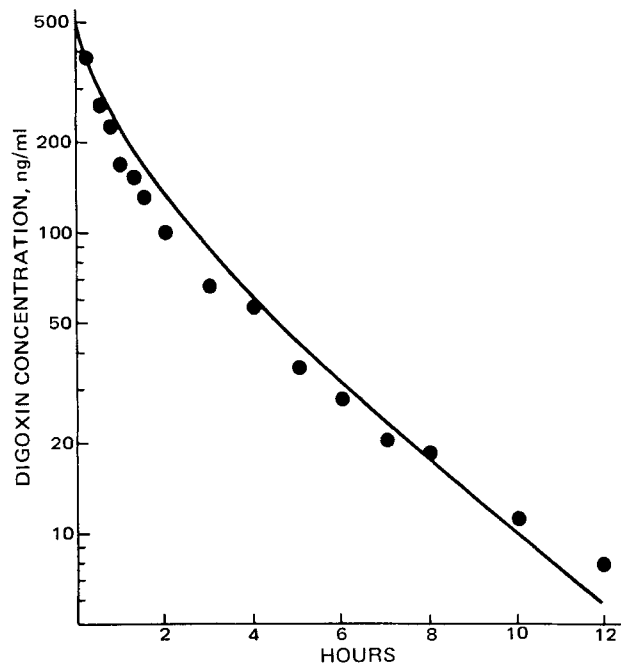

Figure 2—*Predicted (—) and observed (●) plasma digoxin concentrations after a 1-mg/kg iv injection to a bile duct-ligated rat.*

Table I—Steady-State Digoxin Concentrations after a 12-hr Constant-Rate Infusion in Two Rats [a]

Tissue	Experiment	Digoxin Concentration μg/g	μg/Tissue	R_i [b]	Total Radioactivity μg/Tissue	% of Dose
Plasma	1	0.125	—	—	—	—
	2	0.126	—	—	—	—
Liver	1	0.987	12	7.9	13	2.4
	2	0.807	8.3	6.4	9.8	1.8
Skeletal	1	0.171	34[c]	1.4	—	—
muscle	2	0.178	34[c]	1.4	—	—
Heart	1	0.138	0.14	1.1	0.20	<0.1
	2	0.204	0.21	1.6	0.17	<0.1
Kidneys	1	0.213	0.64	1.7	0.98	0.2
	2	0.237	0.67	1.9	0.91	0.2
GI tract	1	9.51	160	76	240	43
	2	6.69	98	53	230	42
Skin	1	—	—	—	12	2.2
	2	—	—	—	9.2	1.7
Carcass	1	—	—	—	50	9.1
	2	—	—	—	57	10
Urine	1	—	89	—	130	23
	2	—	86	—	160	29
Feces	1	—	14	—	15	2.7
	2	—	8	—	17	3.1

[a] Digoxin concentrations were determined by TLC; concentrations of total radioactivity were determined by combustion. [b] Tissue-to-plasma partition coefficients, R_i, were calculated from the ratio of micrograms of digoxin per gram of tissue to micrograms of digoxin per milliliter of plasma at 12 hr. [c] Estimated by assuming that skeletal muscle represents 50% of body weight.

The kidneys and heart showed little ability to concentrate digoxin. These findings in the rat contrast sharply with data from dogs (12) and humans (13), which show kidney-to-plasma and heart-to-plasma ratios of digoxin concentration to be 30 or more. Distribution ratios of digoxin in the heart and skeletal muscle were slightly greater than one. These results are consistent with earlier studies in rats (14, 15).

The mass balance of total radioactivity (Table I) showed that about 83% of the dose was recovered in one rat and about 88% in the other. Digoxin metabolites accounted for about one-half of the total radioactivity. In agreement with previous results in rats (16), almost all radioactivity remaining in the body after the 12-hr infusion was localized in the GI tract. Also, more than 70% of the intact digoxin in the body at 12 hr was found in the GI tract. These results support the notion that biliary and/or GI secretion and enterohepatic cycling play an important role in the distribution of digoxin in the rat (17, 18).

The steady-state distribution of digoxin between the GI tissues and contents in control and bile duct-ligated rats is shown in Table II. The average contents to tissue digoxin concentration ratio was about three in control animals and about two in rats with biliary obstruction. In control animals, this ratio varied from site to site in the GI tract, generally increasing in a distal direction. Ratios of about one in the stomach and small intestine, about three in the cecum, and about eight in the large intestine were found. A similar pattern was not apparent in bile duct-ligated rats. Digoxin concentrations in both the GI tissues and contents were considerably lower in rats with biliary obstruction than in normal rats. Nevertheless, substantial amounts were found in the intestinal contents in the absence of biliary secretion, indicating that GI secretion is a factor in the disposition of the drug in rats.

Pharmacokinetic Model—The experimental observations suggested that the physiologically based model shown in Scheme I could describe the distribution and elimination of digoxin in the rat. This model assumes that: (a) each tissue acts as a well-stirred compartment, (b) drug distribution is plasma flow limited, and (c) all processes are linear, i.e., renal, hepatic, and GI clearances, and tissue-to-plasma partition coefficients are drug concentration independent.

In a single rat, digoxin concentrations in the heart and plasma 12 hr after a 4-mg/kg iv bolus dose of digoxin were four times higher than the concentrations in control rats 12 hr after a 1-mg/kg dose; this finding supports the last assumption. All experimentally observed modes of digoxin elimination in the rat were included in the model, as were GI secretion and enterohepatic circulation of digoxin.
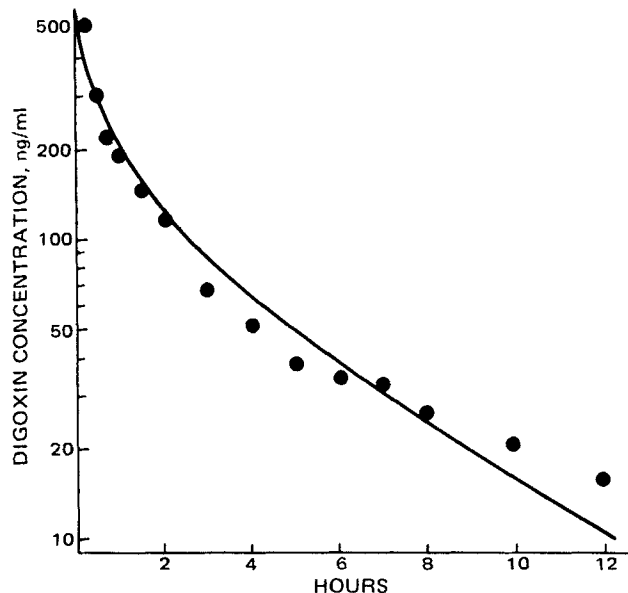

Figure 3—Predicted (—) and observed (●) plasma digoxin concentrations after a 1-mg/kg iv injection to a ureter-ligated rat.
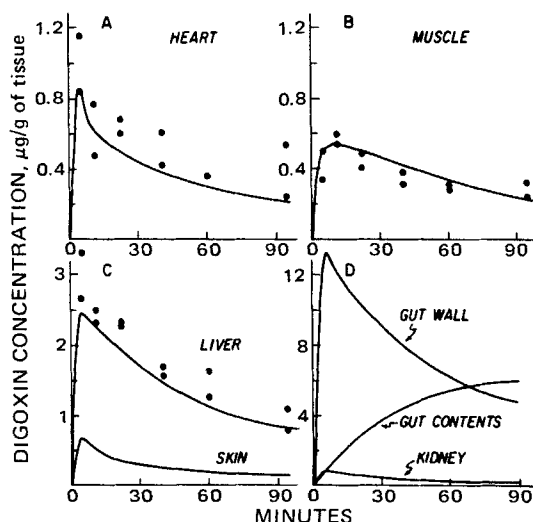

Figure 4—Predicted (—) and observed (●) (n = 2) tissue digoxin concentrations after a 1-mg/kg iv injection to control rats.

Table II—Distribution of Digoxin between GI Tissues and Contents and Corresponding Plasma Concentrations after a 12-hr Infusion in Two Control and Two Bile Duct-Ligated Rats [a]

Tissue	Exper- iment	Digoxin Concentration μg/g	μg/ Tissue	R_i [b]
		Control Rats		
Plasma	1	0.17	—	—
	2	0.12	—	—
GI tissues	1	3.46	25	20
	2	4.11	35	34
GI contents	1	8.58	75	—
	2	11.4	120	—
		Bile Duct-Ligated Rats		
Plasma	1	0.16	—	—
	2	0.14	—	—
GI tissues	1	0.70	5.8	4.4
	2	1.07	4.9	7.6
GI contents	1	1.49	25	—
	2	1.99	24	—

[a] The GI tract was sliced lengthwise, homogenized, and extracted as described for the tissue. [b] Tissue-to-plasma partition coefficient.

A mathematical description of the model is given in the *Appendix*. Organ volumes and plasma flows for a 360-g rat are listed in Table III. Table III also contains the tissue-to-plasma partition coefficients used in testing the model.

Estimates of the various clearance parameters and rate constants are listed in Table IV. Renal clearance was estimated directly in four rats by simultaneous measurement of digoxin concentrations in plasma and urine. A total body clearance of 5.75 ml/min was estimated by dividing the intravenous bolus dose by the area under the plasma digoxin concentration *versus* time curve (9). Since total body clearance was virtually identical in normal and bile duct-ligated rats, it was assumed that this value essentially reflected the sum of renal and hepatic clearances. Therefore, hepatic clearance was estimated by difference. Biliary secretion was calculated from literature data (19).

An initial estimate of GI or fecal clearance of 0.02 ml/min was made by assuming a 12-hr half-life for gut transit (20) and a 20-ml volume for GI contents. Simulations based on this value resulted in an overestimate of digoxin concentrations in the plasma after an intravenous dose to normal rats compared to observed results. After testing several estimates, a value of 0.05 ml/min was selected. The requirement for a higher estimate of GI clearance may indicate that digoxin transit from the absorption site is faster than the average transit of fluid through the gut or that other processes such as gut or bacterial metabolism contribute to the elimination of digoxin from the GI tract.

The first-order absorption rate constant, k_a (Table IV), was obtained by assuming that the absorption half-life of digoxin in the rat is 2 hr (17). The steady-state distribution of digoxin between gut tissues and contents in bile duct-ligated rats (Table II) indicates a ratio of rate constants for gut secretion to gut absorption of about two.

The differential equations listed in the *Appendix* and the constants shown in Tables III and IV served as input for a digital computer analog simulation program (21) to calculate digoxin concentrations in the various model compartments. Modification of these equations to incorporate a zero-order input function yielded predicted steady-state concentrations

Table III—Physiological Constants for the Distribution of Digoxin in the Rat

Tissue	Volume, ml [a]	Plasma Flow, ml/min [b]	R_i [c]
Plasma	10.6	—	—
Heart	2	4.1	1.6
Skeletal muscle	180	8.7	1.4
Skin, fat, *etc.* [d]	90	8.7	1.0 [e]
Kidneys	3.4	14.5	1.9
Liver	13.4	17.4	7.9
GI tissues	10	13.9	30.0
GI contents	17.6	—	—

[a] Based on 360-g rat (20, 22, 23). [b] Total plasma flow = 53.4 ml/min (23–26). [c] Tissue-to-plasma partition coefficient. [d] Miscellaneous compartment for all other body regions. [e] Estimated from total radioactivity data.

Table IV—Clearance and Rate Constants for Digoxin Distribution and Elimination in the Rat

Parameter	Estimate
Renal clearance, K_k	1.25 ml/min
Metabolic clearance, K_l	4.5 ml/min
Biliary clearance, K_b	4.0 ml/min
GI clearance, K_g	0.05 ml/min
Absorption rate constant, k_a	0.006 min^{-1}
Secretion rate constant, k_s	0.012 min^{-1}

of 0.125, 0.2, 0.175, 0.23, 0.98, and 3.75 μg/g for plasma, heart, skeletal muscle, kidney, liver, and GI tissues, respectively. The values are in agreement with the data in Table I and indicate that the model is internally consistent.

Predicted and observed digoxin concentrations in plasma and in liver, heart, and skeletal muscle after a 1-mg/kg iv bolus dose to normal rats are shown in Figs. 1 and 4, respectively. Most model predictions agreed reasonably well with observed values. The predicted and observed plasma digoxin concentrations were compared in three additional control rats, with fits simila: to those seen in Fig. 1. For the first 8 hr, observed plasma concentrations (13 time points/animal) were within 40% of the predicted values.

Excellent agreement was obtained between predicted and observed urinary excretion rates of digoxin for 12 hr after an intravenous bolus dose (Table V).

An attempt was made to extend the pharmacokinetic model developed in normal rats to describe digoxin disposition in rats with cholestasis or with renal failure. The mass balance equations in the *Appendix* were solved simultaneously using all constants in Tables III and IV, except biliary secretion or renal clearance which was set equal to zero. These results were then compared with digoxin concentrations in the plasma of a rat with a ligated bile duct or ligated ureters (Figs. 2 and 3, respectively). Apparently, the same pharmacokinetic model can be used to describe plasma digoxin concentrations in normal rats and in bile duct-ligated or ureter-ligated rats, simply by modifying the appropriate parameters.

The fit of the model was tested in four additional rats: two bile duct ligated and two ureter ligated. In the bile duct-ligated animals, predicted and observed plasma digoxin concentrations were in good agreement, with fits similar to those seen in Fig. 2. For the first 8 hr, the observed plasma concentrations (13 time points/animal) were always within 40% of the predicted plasma concentrations. For the ureter-ligated rats, however, the variability in plasma digoxin levels between animals was too great to allow any correlation of observed and predicted plasma concentrations after 2 hr.

In general, the simulation of cholestasis caused only minor changes in the predicted tissue distribution of digoxin compared to that predicted in normal rats (Fig. 4). Concentrations of digoxin, however, were significantly lower in the GI tissues and contents in the model for cholestasis than in the model for normal rats, in agreement with the distribution data in Table II.

Urinary excretion rates of digoxin for 12 hr after an intravenous bolus dose, predicted by the pharmacokinetic model (modified by assuming a biliary secretion of zero) and observed in bile duct-ligated rats, were compared (Table V). There was good agreement between these data sets.

An important goal in the development of physiologically based pharmacokinetic models in laboratory animals is the potential application to humans simply by scaling blood flows and tissue volumes. This goal was not attainable in these studies, because there are substantial differences in tissue-to-plasma partition coefficients of digoxin between rats

Table V—Comparison of Observed and Predicted Urinary Excretion of Digoxin, Expressed as Percent of Dose, in Control and Bile Duct-Ligated Rats after a 1-mg/kg iv Dose

Hours	Control Rats Observed [a]	Predicted	Bile Duct-Ligated Rats Observed [b]	Predicted
0–4	13.5 ± 4.4	14.2	17.7 ± 8.6	16.5
4–8	2.8 ± 0.6	2.3	4.2 ± 0.9	2.8
8–12	1.1 ± 0.4	0.9	2.0 ± 0.5	0.9
0–12	17.4 ± 4.7	17.4	23.9 ± 8.9	20.2

[a] Mean ± 1 *SD*; n = 5. [b] Mean ± 1 *SD*; n = 6.
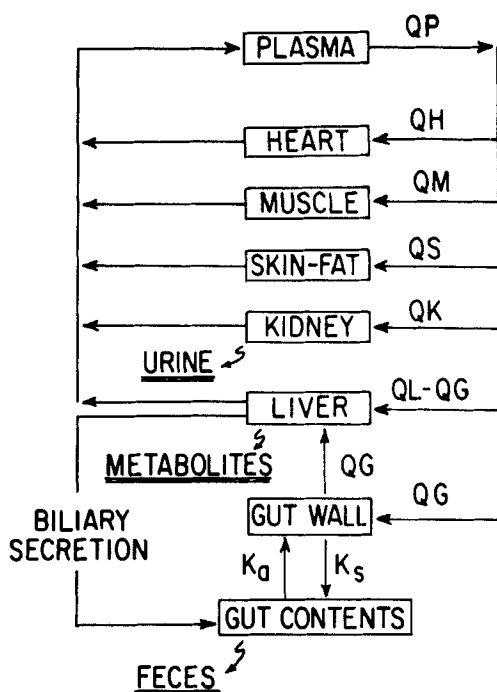
Scheme I—Pharmacokinetic model for digoxin disposition in the rat; QH, QL, QK, etc., denote plasma flow rates to the various organs; QP denotes total plasma flow rate.

and humans (11). The possible application of the present pharmacokinetic model for digoxin to humans using tissue-to-plasma partition coefficients determined in the dog is under investigation.

APPENDIX

The following mass balance–plasma flow equations describe the concentrations in each compartment of the pharmacokinetic model shown in Scheme I:

$$V_p(dC_p/dt) = (Q_hC_h/R_h) + (Q_mC_m/R_m) + (Q_sC_s/R_s)$$
$$+ (Q_kC_k/R_k) + (Q_lC_l/R_l) - Q_pC_p \quad \text{(Eq. A1)}$$

$$V_h(dC_h/dt) = Q_h[C_p - (C_h/R_h)] \quad \text{(Eq. A2)}$$

$$V_m(dC_m/dt) = Q_m[C_p - (C_m/R_m)] \quad \text{(Eq. A3)}$$

$$V_s(dC_s/dt) = Q_s[C_p - (C_s/R_s)] \quad \text{(Eq. A4)}$$

$$V_k(dC_k/dt) = Q_k[C_p - (C_k/R_k)] - (K_kC_k/R_k) \quad \text{(Eq. A5)}$$

$$V_l(dC_l/dt) = (Q_l - Q_g)C_p + (Q_gC_g/R_g) - (Q_lC_l/R_l)$$
$$- (K_lC_l/R_l) - (K_bC_l/R_l) \quad \text{(Eq. A6)}$$

$$V_g(dC_g/dt) = Q_g[C_p - (C_g/R_g)] + k_aV_cC_c - k_sV_gC_g \quad \text{(Eq. A7)}$$

$$V_c(dC_c/dt) = k_sV_gC_g + (K_bC_l/R_l) - k_aV_cC_c - K_gC_c \quad \text{(Eq. A8)}$$

where K_k, K_l, K_b, and K_g represent renal, metabolic, biliary, and GI clearances, respectively; and k_a and k_s represent first-order rate constants for GI absorption and secretion, respectively. The terms V_i, C_i, Q_i, and R_i represent tissue volumes, drug concentrations, plasma flow rates, and tissue-to-plasma partition coefficients, respectively. The subscripts of these terms are as follows: p = plasma; h = heart; m = skeletal muscle,

s = skin, fat, *etc.*; k = kidney; l = liver; g = GI tissues; and c = GI contents.

REFERENCES

(1) K. B. Bischoff and R. G. Brown, *Chem. Eng. Prog. Symp. Ser. No. 66.*, **62**, 33 (1966).
(2) N. Benowitz, R. P. Forsyth, K. L. Melmon, and M. Rowland, *Clin. Pharmacol. Ther.*, **16**, 87 (1974).
(3) *Ibid.*, **16**, 99 (1974).
(4) R. L. Dedrick, *J. Pharmacokinet. Biopharm.*, **1**, 435 (1973).
(5) K. B. Bischoff and R. L. Dedrick, *J. Pharm. Sci.*, **57**, 1346 (1968).
(6) K. B. Bischoff, R. L. Dedrick, D. S. Zaharko, and J. A. Longstreth, *ibid.*, **60**, 1128 (1971).
(7) R. L. Dedrick, D. D. Forrester, J. N. Cannon, S. M. El Dareer, and L. M. Mellett, *Biochem. Pharmacol.*, **22**, 2405 (1973).
(8) B. Montandon, R. J. Roberts, and L. J. Fisher, *J. Pharmacokinet. Biopharm.*, **3**, 277 (1975).
(9) L. I. Harrison and M. Gibaldi, *Drug Metab. Dispos.*, **4**, 88 (1976).
(10) F. I. Marcus, A. Peterson, A. Salel, J. Scully, and G. G. Kapadia, *J. Pharmacol. Exp. Ther.*, **152**, 372 (1966).
(11) J. E. Doherty, W. H. Perkins, and W. J. Flanigan, *Ann. Intern. Med.*, **66**, 116 (1967).
(12) J. E. Doherty and W. H. Perkins, *Am. J. Cardiol.*, **17**, 47 (1966).
(13) K. E. Anderson, Å. Bertler, and G. Wettrell, *Acta Paediatr. Scand.*, **64**, 497 (1975).
(14) S. Dutta and H. Marks, *Life Sci.*, **5**, 915 (1966).
(15) V. K. Buchetala, H. Hackel, M. Königstein, and J. Schläger, *Wien. Med. Wochenschr.*, **118**, 86 (1968).
(16) G. T. Okita, *Fed. Proc.*, **26**, 1125 (1967).
(17) N. Rietbrock, U. Abshagen, K. v. Bergmann, and H. Kewitz, *Naunyn Schmiedebergs Arch. Pharmacol.*, **274**, 171 (1972).
(18) U. Abshagen, K. v. Bergmann, and N. Rietbrock, *ibid.*, **275**, 1 (1972).
(19) J. Q. Russell and C. D. Klaassen, *J. Pharmacol. Exp. Ther.*, **186**, 455 (1973).
(20) R. C. Thompson and O. L. Hollis, *Am. J. Physiol.*, **194**, 308 (1958).
(21) "MIMED, State University of New York at Buffalo Computer Center Adaptation of MIMIC," Publication 44610400, Control Data Corp., St. Paul, Minn., 1968.
(22) E. F. Adolph, *Science*, **109**, 579 (1949).
(23) L. Jansky and J. S. Hart, *Can. J. Physiol. Pharmacol.*, **46**, 653 (1968).
(24) Y. Sasaki and H. N. Wagner, *J. Appl. Physiol.*, **30**, 879 (1971).
(25) L. A. Sapirstein, E. H. Sapirstein, and A. Bredemyer, *Circ. Res.*, **8**, 135 (1960).
(26) L. Takács, K. Kállay, and V. Vajda, *Acta Physiol. Acad. Sci. Hung.*, **21**, 87 (1962).